Proc. Natl. Acad. Sci. USA
Vol. 80, pp. 609–621, January 1983
Review

Influence of nuclear spin on chemical reactions: Magnetic isotope and magnetic field effects (A Review)

(spin dynamics/photochemistry/radical pairs/isotope enrichment)

NICHOLAS J. TURRO

Department of Chemistry, Columbia University, New York, New York 10027

Contributed by Nicholas J. Turro, November 1, 1982

ABSTRACT **The course of chemical reactions involving radical pairs may depend on occurrence and orientation of nuclear spins in the pairs. The influence of nuclear spins is maximized when the radical pairs are confined to a space that serves as a cage that allows a certain degree of independent diffusional and rotational motion of the partners of the pair but that also encourages reencounters of the partners within a period which allows the nuclear spins to operate on the odd electron spins of the pair. Under the proper conditions, the nuclear spins can induce intersystem crossing between triplet and singlet states of radical pairs. It is shown that this dependence of intersystem crossing on nuclear spin leads to a magnetic isotope effect on the chemistry of radical pairs which provides a means of separating isotopes on the basis of nuclear spins rather than nuclear masses and also leads to a magnetic field effect on the chemistry of radical pairs which provides a means of influencing the course of polymerization by the application of weak magnetic fields.**

PHYSICAL MODEL OF NUCLEAR SPIN

"Spin" is the term used to describe an intrinsic and characteristic property associated with the angular momentum of a particle. A physical model of spin is conveniently generated by the supposition that this property is the angular momentum that arises from a body rotating about its own axis. This classical model allows recognition of most of the important characteristics of quantum mechanical spin. For example, it provides an understanding of why charged particles with spin possess an intrinsic magnetic moment and why charged particles without spin do not possess an intrinsic magnetic moment (1, 2) (Fig. 1).

The magnitude of the spin angular momentum of a particle is uniquely determined by the spin quantum number which may be a positive integral or half-integral number that is characteristic of the particle. For example, the value of the electronic spin quantum number(s) for an electron is $+1/2$. This value pertains whatever the state of the electron. On the other hand, the value of the nuclear spin quantum number (ℓ) depends on the nucleus. Indeed, some nuclei (e.g., ^{12}C, ^{16}O, ^{18}O) do not possess spin ($\ell = 0$), whereas others possess half-integral values (e.g., for ^{17}O $\ell = 5/2$, for ^{1}H $\ell = 1/2$, and for ^{13}C $\ell = 1/2$) or integral values (e.g., for ^{2}H $\ell = 1$). For simplicity, I shall consider some of the consequences of a simple model of spin for a particle with spin quantum number of $+1/2$.

According to the rules of quantum mechanics, the spin angular momentum of a rotating body is quantized and may take up only a discrete set of orientations with respect to any arbitrarily selected axis (Fig. 2). With the z axis as a frame of reference, the allowed orientations for a spin of $+1/2$ are "up" (α spin) and "down" (β spin). Quantum mechanics allows that only one axial component of the spin angular momentum vector can be specified. We shall arbitrarily select this component to be projected on the z axis. The specific orientation (termed the "azimuth") of the vector in the xy plane cannot be determined precisely according to the rules of quantum mechanics because the uncertainty principle requires that, if the z component of the angular momentum is precisely specified, then the x and y components cannot be specified. The range possible for orientations of the angular momentum vector in the xy plane traces out a cone which is termed a "cone of precession for the vector." The magnetic moment vector that is associated with the spinning charged particle behaves qualitatively in the same manner as the angular momentum vector. The magnetic moment is influenced by magnetic fields due to nearby spins and by applied magnetic fields.

In the absence of other magnetic fields, the magnetic moment vector may be viewed as being at rest at an indeterminate position in the cone of precession and may assume any orientation in space. If a magnetic field H is applied along the z axis, the spin vectors must take up either the α or β position (Fig. 2). The vector is now viewed as revolving about the z axis with

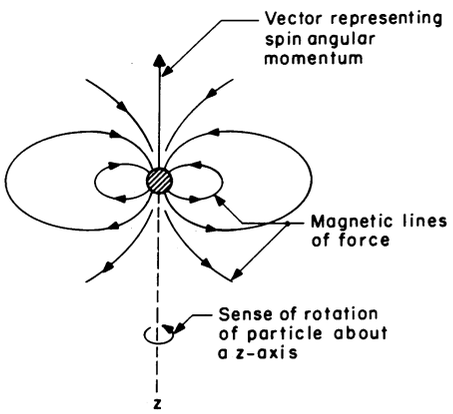

FIG. 1. Schematic description of classical spin angular momentum of a rotating particle. The spin angular momentum can be represented as vector quantity whose magnitude is interpreted as the angular momentum resulting from the spin and whose direction represents the sense of the rotation. A particle with both mass and charge generates a magnetic field as it spins. This field can also be represented by a vector quantity, a magnetic moment. In the case of a charged particle, the "right-hand rule" applies for a positively charged particle (atomic nucleus) for both the direction of the angular momentum and the magnetic moment vectors. In the case of a negatively charged particle (electron), the magnetic moment vector is opposite in direction to the angular momentum vector. The orientation in space of a classical magnetic moment can assume any value relative to an applied magnetic field, but the magnetic moment of an electron or a nucleus in an external magnetic field is only allowed a few orientations as specified by the laws of quantum mechanics.

Abbreviations: ISC, intersystem crossing; RP, radical pairs; DBK, dibenzyl ketone; $C_{16}NMe_3Cl$, hexadecyltrimethylammonium chloride; CMC, critical micelle concentration.

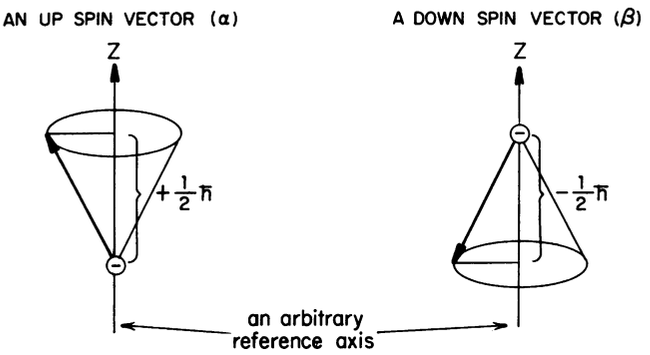

FIG. 2. Vector representation of the two possible orientations of the magnetic moment of a charged particle with spin 1/2 in an external field or relative to an arbitrary z axis. The absolute magnitude ($\hbar/2$) of the component of the magnetic moment in the direction of the field is the same for the "up" (α) or the "down" (β) situation but is opposite in sign—i.e., the allowed values of the angular momentum along the z axis are $\mathcal{J}_z = +\hbar/2$, and $\mathcal{J}_z = -\hbar/2$. From the laws of quantum mechanics the vectors may lie in either of two cones, as shown.

a precessional frequency ω. The value of ω is proportional to the magnitude of H, where μ is the magnetic moment associated with the spinning charged particle.

$$\omega \alpha \mu H \qquad [1]$$

The vector model and Eq. 1 reveal that the rate of precession about the x axis is directly related to the strength of coupling to the magnetic field along the z axis. These ideas are readily extended to more complex situations where several magnetic fields applied in different directions actively compete to serve as the axis about which the magnetic angular momentum will precess. Thus, we can expand the concept of an up-spin and a down-spin with a precessing up-spin or a precessing down-spin.

The interactions of electron and nuclear spin magnetic moments: The kinetic magnetic isotope effect

It is the interaction of magnetic moments of nuclei with the magnetic moments of electrons (termed the "nuclear–electronic hyperfine coupling") that provides a vehicle for nuclear spins to influence chemical reactions. These interactions are so tiny (Table 1) that they have no significant influence on equilibrium properties of chemical systems but in certain situations they serve as a means of modifying the rates of chemical reactions. Indeed, the hyperfine interactions cause the appearance of a novel isotope effect on chemical reactions—the kinetic magnetic isotope effect (3, 4)—which allows the chemical reactions of isotopes possessing different nuclear spins to proceed at different rates. We now ask What are the conditions under which the magnetic isotope effect may be magnified and be observed as a significant experimental result? In other words, Under what circumstances can nuclear spins significantly influence the pathways of chemical reactions?

Table 1. Conversion table for magnetic field effects

	Magnetic induction, G	cm^{-1}	Energy, kcal/mol
Very strong magnet	100,000	10	10^{-2}
Strong magnet	10,000	1	10^{-3}
Toy magnet, strong hf	100	10^{-2}	10^{-5}
Typical hf	10	10^{-3}	10^{-6}
Earth's magnetic field	1	10^{-4}	10^{-7}
Chemical bond	2×10^8	20,000	59

In most chemical reactions, each elementary chemical step along a reaction pathway proceeds without overall change in the intrinsic angular momentum of the electron spins—i.e., the spins of electrons are paired and conserved throughout the reaction sequence. In certain reactions, however, orbital uncoupling of electrons occurs and the chemical effects of electron spins become more likely.

It is natural to seek magnetic spin effects in reactions producing or destroying radicals because such reactions involve the production or destruction of net magnetic moments of electrons, and electrons interact strongly with themselves, with the magnetic moments of nuclei, and with applied laboratory magnetic fields.

A radical pair (RP) is a simple example of a system for which transitions commonly occur between electronic levels of different electronic multiplicity (different net magnetic character) and without conservation of electronic spin. When correlated, the electronic spins of the two unpaired electrons may orient (Fig. 3) in a manner that either cancels completely, corresponding to a multiplicity of zero (the singlet state of the RP), or adds up to a value corresponding to a multiplicity of unity (the triplet state of the RP). The state with a net electronic spin of 0 is termed a "singlet state" because it remains a single state in the presence of a magnetic field. The state with a net electronic spin of 1 is termed a "triplet state" because the total electron spin may be oriented, according to the laws of quantum mechanics, in three different ways in a magnetic field—i.e., the total spin vector may take up three orientations in space (projections on the z axis termed +1, 0, and −1 as shown in Fig. 3). These three sublevels of the triplet state are termed T_+, T_0, and T_- for the situations in which both individual electron spins are "up," one spin is "up" and one spin is "down," and both spins are "down," respectively.

Singlet–triplet and triplet–singlet intersystem crossings (ISCs) in the RP under certain conditions may be induced by hyperfine electron–nuclear interactions which cause simultaneous exchanges in nuclear and in electron spin. In this way, nuclear spins, through the hyperfine interactions, can influence the rate of ISC in a RP and, as a consequence, also can influence the probability or efficiency in the self-reactions of pair because the self-reactions available to the RP (recombination and disproportionation) can only take place in the singlet pair.

The nuclear spin isotope effect (or, as it has also been termed, "the magnetic isotope effect") results from the different rates of ISC between "magnetic" and "nonmagnetic" RPs (or, more generally, between RPs possessing different magnetic moments) and from the resulting different probability of combination of the pairs. The ratio of rates of combination of radicals for magnetic and nonmagnetic pairs provides a quantitative measurement of the magnetic isotope effect.

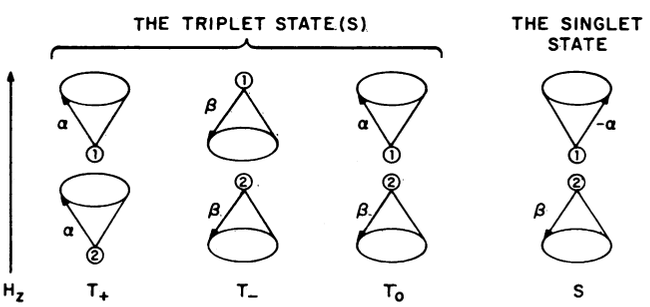

FIG. 3. Schematic vector representation of a triplet state and a singlet state. The difference between α and $-\alpha$ is intended to reflect a "phase" difference of 180°.

Conditions for non-conservation of spin angular momentum in radical reactions

The intrinsic spin angular momenta possessed by electrons and nuclei can be expected to exert dramatic influences on the rates of chemical reactions only under conditions such that the usual laws for conservation of angular momenta break down. The total spin angular momentum of electrons and nuclei is faithfully preserved for the elementary steps of all radical reactions involving homolytic transfer. The "goodness" of the spin conservation laws is related in part to time scales. An elementary chemical step typically requires $\approx 10^{-12}$ to 10^{-13} sec for completion (time period of nuclear vibrational reorganizations). There is little chance for alternation of the electronic or nuclear spin momentum during such a short time period. In effect, the rephasing of the vectors representing electronic or spin angular momentum is very slow relative to nuclear motion. The Franck–Condon principle states that electronic orbital motion is much faster than nuclear motion, so that nuclear spatial configurations are fixed during electronic reorganizations—i.e., during the time of an electronic transition, the initial and final nuclear spatial configurations are identical. Of course, after the electronic transition has been completed, the nuclei will readjust to the new electronic potential in which they are immersed and (in general) a new nuclear configuration will result.

Wigner's selection rules for conservation of spin angular momenta during chemical reaction can be viewed in a manner analogous to the Franck–Condon principle: during the time period of a typical elementary chemical step, the spin angular momentum changes much more slowly than the electronic or nuclear spatial reorganizations; therefore, the initial and final spin angular momenta are identical for an elementary chemical process.

It is now apparent that there may be general situations for which the spin angular momenta may not be conserved in radical reactions—e.g., for "long-lived" states. In such situations, the life-times of radicals are long enough to allow the spin angular momentum vectors "to move" and to follow electronic and nuclear spatial reorganizations. A further requirement is that any change in spin angular momentum must be compensated for in detail by some other momentum exchange in the system. For example, if a change in spin multiplicity (e.g., a triplet-to-singlet ISC) can occur along with the change in nuclear spin, overall conservation laws may be obeyed.

At this point it may be clear that, in order to find systems for which nuclear spins influence the pathways of chemical reactions, it is necessary to consider three kinds of time-dependent processes: (*a*) the chemical dynamics of the reacting system, which cannot be too fast (or the spin angular momenta will be faithfully conserved) or too slow (or the spin angular momenta will be randomly dispersed); (*b*) the spin dynamics of the interaction electron and nuclear magnetic moments (which depend on rates of precession of the various spin momenta vectors and their orientations in space); (*c*) the molecular dynamics of diffusion and rotation of the reacting species (which may influence directly both the rates of chemical processes and spin momenta exchanges). With this background we are now ready to expound a program for identifying concrete examples of reactions that may be influenced by nuclear spins.

REACTIONS THAT MAY BE INFLUENCED BY NUCLEAR SPINS

Nuclear spin-dependent mechanisms for ISC of a RP

The mechanisms by which nuclear spins can operate to influence the rate of ISC of a triplet RP are shown schematically in Figs. 4 and 5. The electron spin vectors are assumed to be weakly coupled to each other but strongly coupled to some magnetic field $\vec{H}$. Two mechanisms for ISC are suggested by the vector model of the singlet and triplet states: (*i*) a spin "rephasing" mechanism by which T_0 and S (each of which possesses one α spin and one β spin and which differ only in the azimuth angle) can be interconverted; (*ii*) a spin-flip mechanism by which T_+ (or T_-) and S can be interconverted.

The interconversion of T_0 and S only requires the rotation of one of the electron spin vectors relative to the other about the *z* axis. In the absence of an applied laboratory field, the net magnetic field experienced by electron 1 and electron 2 spin vectors in the *z* direction is the sum of internal fields arising from nearby nuclear spins and electron orbital motion. If a laboratory

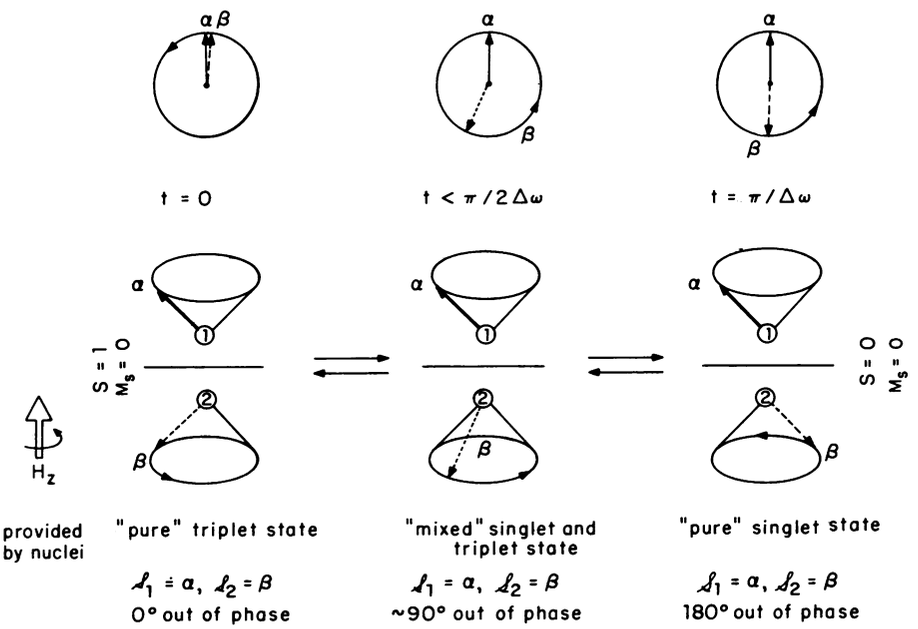

FIG. 4. Rephasing mechanism for ISC. A magnetic field, H_z, provides a torque on $\mathcal{H}_2$ to cause it to precess at a different rate than $\mathcal{H}_1$. As a result, after a period of time $\pi/\Delta\omega$, a triplet state evolves into a singlet state. No "spin flips" of electrons or nuclei are involved in this mechanism.

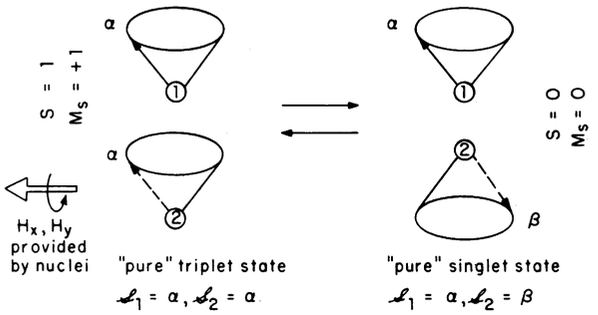

FIG. 5. Spin-flipping mechanism for ISC. A magnetic field (H_x or H_y) provides a torque that causes the $\mathcal{S}_2$ vector to flip from an α to a β orientation. If H_x or H_y is provided by magnetic nuclei, a nuclear spin flip occurs simultaneously with the electron spin flip.

field $\tilde{H}_0$ is applied, there will be a competition set up in which the internal fields and the applied field compete for magnetic control of the orientation and precession of the electron spin vectors. In general, the difference between precessional frequencies ($\Delta\omega$) of the spin vectors will be given by

$$\Delta\omega = (\beta/\hbar)[\Delta g H_0] + \Delta\Sigma a_i m_i \qquad [2]$$

where $\Delta g H_0$ arises from the Zeeman interaction for cases in which the g factors of the two electrons are different and $\Delta\Sigma a_i m_i$ arises from the difference in the hyperfine field experienced by electrons where a is the pertinent hyperfine interaction and m is the pertinent magnetic quantum number.

The projection of the electron spins in the xy plane is shown at the top of Fig. 4. For the T_0 state this projection shows the vectors superimposed (i.e., separated by an angle $\theta = 0°$), and for the S state this projection shows the vectors separated by 180°. The rate of ISC for the rephasing of T_0 to S will depend on the differences of both the g factors of electron 1 and electron 2 and the hyperfine fields experienced by spins—i.e., ISC between T_0 and S will be determined by an applied field dependence and a nuclear spin dependence. If $\Delta g = 0$, or if $\tilde{H}_0 = 0$, only the nuclear spin dependence will operate.

The interconversion of T_+ (or T_-) to S involves the flip of an electron spin vector (Fig. 5). The "torque" serving as a force to flip the electron spin vector will come from magnetic fields in the xy plane. If these fields are associated with the hyperfine interaction, then a nuclear spin flip can be coupled with an electron spin flip to conserve the total angular momentum of the system—i.e., under conditions of a simultaneous nuclear–electron spin flip, T_+ (or T_-) to S interconversions are completely allowed. It may be appreciated that the $[T_+, T_-] \rightleftarrows$ S ISC takes a relatively long time because the system must "search," via diffusional and rotational displacements of the radical fragments, for structural geometries that allow for the hyperfine interaction to be effectively utilized.

Surface description of the homolytic cleavage of a molecule T_0 for a spin-correlated RP

Consider Fig. 6 which shows schematically the energy variation of the lowest singlet and triplet states of a molecule, a—b, as a function of increasing separation of the fragments into the free radicals a + b. In region I the bond is severely weakened and the energy gap between the S and T states begins to decrease rapidly as the bond is increased further. In region II, the bond between a and b is completely broken. This means, operationally, that the molecular motions of the two radicals a and b no longer are constrained by the occurrence of the bond. However, the motions of the radicals are constrained by the "cage" or the

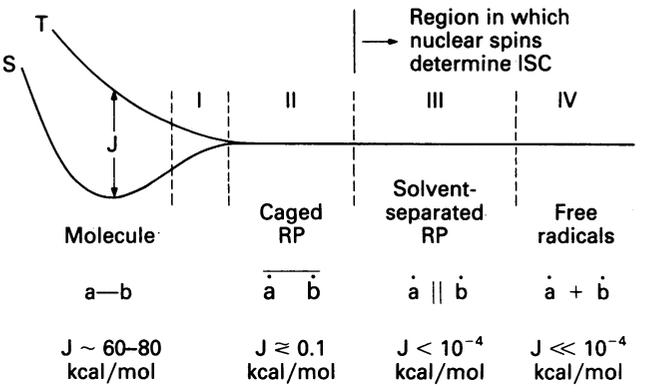

FIG. 6. Schematic representation of the exchange interaction, J, of an electron pair initially localized in a bond between groups a and b and then localized as odd electrons on a and b. The effect of J is to split T from S energetically and thereby inhibit ISC.

environment in which they are created. In a nonviscous solvent, the "solvent cage" provides a weak constraint to diffusional separation and very little constraint to rotational motion. In region III, the radicals are separated by one or several solvent molecules and their diffusional motions are essentially independent of one another. However, statistically there is a relatively high probability that the solvent-separated geminate pair will reencounter in a solvent cage at least once. In region IV, the radical fragments have diffused to positions in space such that all compositional correlation is randomized—i.e., a and b have become true free radical fragments. The situation at "large" separations of a and b (regions III and IV) is such that the S and T states are "touching" in the sense that their energetic separation is comparable or small relative to hyperfine energies, a feature that is crucial for the operation of spin effect.

Consider now the trajectory of a representative point that tracks the progress of bond breaking and the separation of the fragments (Fig. 7). If the representative point starts on the triplet surface, it experiences a repulsive force that drives it to the right—i.e., toward bond breaking. The momentum provided by this force will tend to cause a and b to continue to separate. The point will remain on the triplet surface even in the touching region. If nuclear spins assist in ISC from the triplet surface to the singlet surface and if the direction of the momentum of the representative point can be reversed to the left—i.e., toward bond-making—stable singlet molecules will be formed and these molecules will be enriched in the nuclear states that assisted in the ISC process, if an "escape" route is available for radical pairs that do not possess hyperfine interactions.

In the absence of any perturbing magnetic fields, the two orbitally uncoupled spins on a and b will remain at some indefinite overall orientation in space but will maintain a well-

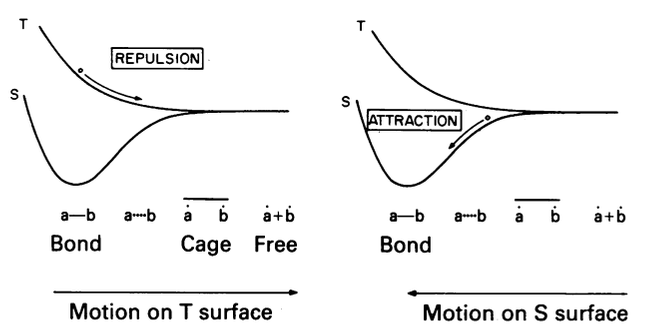

FIG. 7. Motion of a representative point on a dissociative triplet surface (*Left*) and on an attractive singlet surface (*Right*).

defined relative orientation of one of the triplet levels. In the presence of magnetic fields the electron spins will precess about a direction that is determined by the strengths of the available fields. If the fields are identical for the two separated electron spins, their precessional rates and relative orientations will remain identical—i.e., the electronic spin character of the pair will not change. If, however, the fields operating on the two spins are different, the rates of precession of the individual spins will differ if the field operates perpendicular to the x or y axis, and the triplet phasing will be lost or one of the electron spins may be turned over or flipped (if the field operates perpendicular to the z axis).

The interplay of spin dynamics, molecular dynamics, and chemical dynamics: Influence on the rate and efficiency of ISC of a RP

The spin dynamics of a RP (hyperfine-induced ISC) and the molecular dynamics of a RP (diffusional and rotational displacements in space) cannot be treated independently in general. The diffusional motions lead to an array of average separations of the odd electron centers and the rotational motions lead to time-dependent relative structural orientations of the fragment. Thus, diffusion and rotation modulate the (distance and orientation dependent) exchange interaction between the radical fragments in the RP. Because the exchange interaction determines the singlet–triplet splitting, any dynamic features that modulate the exchange interaction will also modulate the singlet–triplet splitting and, in turn but indirectly, will also modulate the rate of ISC in the RP.

The chemical dynamics of the RP also enter the efficiency of ISC of a RP. Because ISC is typically a relatively slow process, the RP must preserve its chemical integrity during the time period required for ISC to occur. An irreversible chemical reaction may destroy the RP (via self-reaction) or modify one or both of the radicals (via independent reactions of the individual radicals to produce a new RP). Thus, unless ISC can occur before an irreversible chemical reaction destroys or modifies the RP, the efficiency of ISC of the initial RP is decreased. On the other hand, if a RP is formed reversibly, the chemical dynamics provide an opportunity to enhance the nuclear spin isotope effect by providing an escape route for the pairs for which nuclear spins cannot promote ISC. This can be seen in the following example. Suppose the triplet RP $^3\dot{a}\dot{b}$ experiences a competition between nuclear spin-induced ISC to $^1\dot{a}\dot{b}$ and a chemical reaction that does not depend on nuclear spin. If $^1\dot{a}\dot{b}$ efficiently reacted to regenerate a—b, then a means of separating molecules of a—b, based on nuclear spins, is available.

Isotopic separations based on nuclear spins

The reactivity of a RP within a solvent cage ($\overline{RP}$) depends critically on the spin state of the pair. As a general rule, a singlet RP ($^1\overline{RP}$) within a solvent cage is very reactive toward combination and disproportionation reactions, whereas triplet RPs in a solvent cage ($^3\overline{RP}$) are completely unreactive toward such reactions. The options open to a $^3\overline{RP}$ in a chemically inert solvent are (*a*) chemical modification of one (or both) of the components of the pair to produce a structurally different triplet radical, (*b*) relative diffusion of the pair out of the solvent cage, and (*c*) ISC to produce a reactive singlet RP. The general rule concerning the differing reactivities of $^1\overline{RP}$ and $^3\overline{RP}$ is based on the premise that the time of reaction of a caged RP is too short for a change of electronic spin multiplicity.

(*a*) $^1\overline{RP} \rightarrow$ disproportionation or combination or both

(*b*) $^3\overline{RP} \rightarrow {}^3\overline{RP}'$ or $\dot{a} + \dot{b}$

(*c*) $^3\overline{RP} \rightarrow {}^1\overline{RP}$

Path *b* provides an escape pathway for pairs that do not possess magnetic spins and path *c* provides a capture for the pairs that possess magnetic spins. A strategy for controlling the reactions of RPs with nuclear spins can now be developed. If the nuclear spins communicate with the electron spin via nuclear–electronic hyperfine-induced ISC of a RP, then reactivity of the RP will depend on the nuclear–electronic hyperfine coupling. As a general example, consider two RP precursors, a*—b and a—b, that differ only in isotope substitution (Fig. 8) (* refers to the occurrence of magnetic nuclei in a fragment of the RP). Suppose now that both precursors are cleaved into a caged triplet RP, $^3\overline{a^*b}$ and $^3\overline{ab}$, respectively. Of the two, $^3\overline{a^*b}$ will convert more rapidly into singlet $^1\overline{a^*b}$ because the magnetic nuclei in a^* provide a mechanism for ISC that is completely absent in $^3\overline{ab}$. If a singlet RP undergoes a cage recombination reaction, then a*—b will be reformed faster than a—b. This means that as the reaction proceeds, the system will become enriched in the reagent containing magnetic nuclei. In principle, such a system could lead to complete separation of the isotopic materials of a*—b and a—b, if the escape process occurred for all pairs that did not contain magnetic spins and if the capture process occurred for all pairs containing magnetic spins.

For efficiency, however, two important criteria must be met: (*i*) the hyperfine interactions in the caged RP $^3\overline{a^*b}$ must be large enough to allow for the possibility that ISC crossing to $^1\overline{a^*b}$ can be determined mainly by nuclear spins, and (*ii*) the formation of free radical products (chemical or modification of the RP) from $^3\overline{ab}$ must occur more efficiently than ISC to $^1\overline{ab}$. In turn, in order for these criteria to be met, certain space/time conditions must exist: (*a*) the caged RP $^3\overline{a^*b}$ must be able to use the hyperfine interactions fully by being able to have the radical fragments separate in space to a distance such that the singlet–triplet splitting is of the order of or smaller than the hyperfine interaction and (*b*) the time of separation must be appropriate for maximal ISC induced by hyperfine interactions.

Thus, the probability of triplet–singlet ISC of a RP and hence the probability of reaction of the RP depends on the occurrence of nuclear spins and on the spin orientations of the magnetic

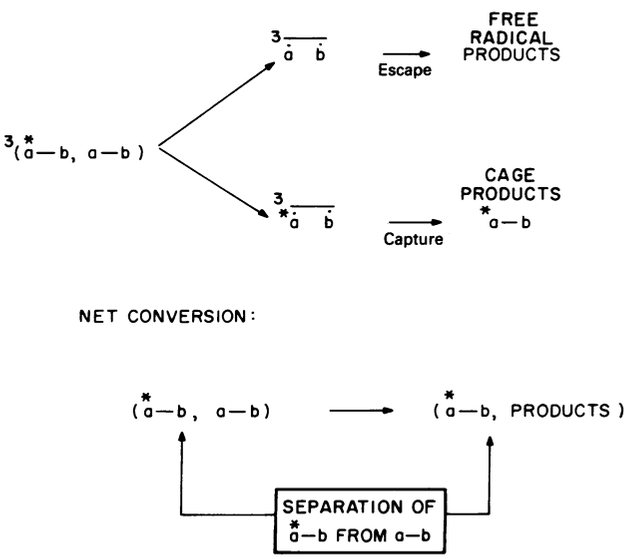

FIG. 8. Scheme for separation of a fragment containing magnetic isotopes (a*) from a fragment containing nonmagnetic isotopes (a).

nuclei in the pair. As a consequence, the combination or capture products may be enriched (or impoverished) in nuclear spins or nuclear spins of a certain orientation—i.e., a nonequilibrium or polarized population of nuclear Zeeman levels is produced in the combination products. This phenomenon is known as "chemically induced dynamic nuclear polarization (CIDNP)." Furthermore, the probability of combination reaction of a triplet RP depends on the hyperfine electron–nuclear interactions, so that RPs possessing nuclei of isotopes with different magnetic moments will have combination probabilities that are related to the hyperfine coupling of the nuclear magnetic moments to the electron magnetic moments.

For example, it could be imagined that triplet RPs containing a magnetic isotope (e.g., ^{13}C) undergo more rapid ISC than RPs containing nonmagnetic isotopes (e.g., ^{12}C). As a result, singlet pairs containing magnetic isotopes form more rapidly and hence self-reactions involving magnetic isotopes occur with a more rapid rate and a higher probability (if an escape reaction or process is available to the nonmagnetic pairs). I shall now review the experimental results that demonstrated the feasibility of separation of ^{13}C- from ^{12}C-containing molecules via the magnetic isotope effect.

EXPERIMENTAL RESULTS

Photolysis of dibenzyl ketone: A paradigm system for investigation of the influence of nuclear spins on the reactions of RPs

The photochemistry of dibenzyl ketone (DBK) has provided an excellent basis for exploration and demonstration of the influence of nuclear spins on the reactions of RPs. The overall reaction (Eq. 3) leads to quantitative yield of 1,2-diphenylethane (DPE) and CO.

$$\underset{\text{DBK}}{C_6H_5CH_2COCH_2C_6H_5} \xrightarrow{h\nu} \underset{\text{DPE}}{C_6H_5CH_2CH_2C_6H_5} + CO. \quad [3]$$

The "classical" mechanism for photolysis of DBK in typical nonviscous organic solvents is:

$$C_6H_5CH_2COCH_2C_6H_5 \xrightarrow{h\nu} S_1 \quad [4]$$

$$S_1 \rightarrow T_1 \quad [5]$$

$$T_1 \rightarrow \overline{C_6H_5CH_2\dot{C}O\ \dot{C}H_2C_6H_5} \quad [6]$$

$$^3RP \rightarrow C_6H_5CH_2\dot{C}O + C_6H_5\dot{C}H_2 \quad [7]$$

$$C_6H_5CH_2\dot{C}O \rightarrow C_6H_5\dot{C}H_2 + CO \quad [8]$$

$$2\,C_6H_5\dot{C}H_2 \rightarrow C_6H_5CH_2CH_2C_6H_5. \quad [9]$$

The initial act of absorption produces a n,π^* excited singlet state (S_1) which undergoes a radiationless transition to a lower-lying n,π^* triplet state (T_1). The latter then undergoes homolytic cleavage (Eq. 6) to produce a geminate ^3RP in a solvent cage (the bar over the pair indicates a solvent cage). In homogeneous, nonviscous solvents (benzene, acetonitrile), ^3RP undergoes quantitative formation of free radicals (Eq. 7). The free $C_6H_5CH_2\dot{C}O$ radical undergoes quantitative decarbonylation (Eq. 8). Finally, random free $C_6H_5\dot{C}H_2$ radicals produced in Eq. 7 or in Eq. 8 combine to produce diphenylethane (Eq. 9).

The time scale for formation of free radicals (Eq. 7) is of the order of 10^{-10} to 10^{-11} sec in benzene or acetonitrile. This time scale is too short to allow hyperfine interactions to promote a change in spin angular momentum. As a result, nuclear spins do not have an opportunity to influence the ISC of ^3RP.

From the principles put forth earlier, in order to create a situation that is favorable for the influence of nuclear spins on some of Eqs. 7–9 the following are necessary but not sufficient requirements: (*i*) the triplet correlation of ^3RP must be preserved for a sufficient period of time ($\gtrsim 10^{-9}$ sec) for hyperfine interactions to promote ISC to a singlet RP (^1RP); (*ii*) the hyperfine induced ISC must be significant mechanism for the $^3RP \rightarrow {}^1RP$ process; and (*iii*) ^3RP must have an alternate competitive escape pathway which does not depend on nuclear spins.

As an example, consider:

$$\underset{^3RP}{\overline{C_6H_5CH_2\dot{C}O\ \dot{C}H_2C_5H_6}} \rightarrow \underset{^1RP}{\overline{C_6H_5CH_2\dot{C}O\ \dot{C}H_2C_6H_5}} \quad [10]$$

$$\underset{^3RP}{\overline{C_6H_5CH_2\dot{C}O\ \dot{C}H_2C_6H_5}} \rightarrow \underset{^3RP'}{\overline{C_6H_5\dot{C}H_2}} + CO + C_6H_5\dot{C}H_2 \quad [11]$$

$$^1RP \rightarrow C_6H_5CH_2COCH_2C_6H_5. \quad [12]$$

Eqs. **10** and **11** represent competitive processes of an electron spin-correlated RP: ISC whose rate is (in principle) dependent on nuclear spins, and decarbonylation which does not involve a change in magnetic properties and whose rate should therefore not depend on nuclear spins. However, in homogeneous solution, neither Eq. **10** nor Eq. **11** occurs efficiently because escape from the solvent cage and formation of free radicals is the process which "destroys" the correlated pair, ^3RP.

Evidently, because the cage environment provided by homogeneous, nonviscous, solvent is too "weak" to contain ^3RP for a sufficiently long period of time, a much "stronger" or "super" cage environment is required to allow the competitive steps, Eqs. **10** and **11**, to operate. The requirements of such an environment are that the fragments of ^3RP be allowed to execute diffusional and rotational motions that will decrease J (electron exchange energy) to a value comparable to or smaller than that of the hyperfine energies associated with the radical fragments in the pair. The environment must allow and encourage ^1RP to undergo combination reaction(s) after ISC.

An environment that meets these requirements is provided by the hydrophobic interior and surface of micelle aggregates which form in aqueous solutions of ionic detergents.

Micellar aggregates from aqueous solution of detergents

The structure of a detergent molecule typically is partially hydrophobic and partially hydrophilic (5, 6). For instance, ionic detergents commonly have a straight chain hydrocarbon "tail" consisting of 10–18 carbon atoms terminating in an ionic "head." Hexadecyltrimethylammonium chloride ($C_{16}NMe_3Cl$), $CH_3(CH_2)_{15}\overset{+}{N}(CH_3)_3Cl^-$, is an example of a cationic detergent and sodium dodecylsulfate, $CH_3(CH_2)_{11}OSO_3^-Na^+$, is an example of a anionic detergent. When added to water at low concentrations, these detergents form solutions that have the properties expected for solutions of simple electrolytes. Above a certain concentration (that depends on the detergent structure) many of the properties (i.e., viscosity, light scattering, electrical conductance) of the solution deviate sharply from those expected for solutions of simple electrolytes.

The concentration (or range of concentrations) for which the properties of detergent solutions begin to show sharp deviation from the behavior of simple electrolytes is called the "critical micelle concentration" or CMC because at this concentration detergent molecules begin to aggregate to form micelles. Fig. 9 shows a schematic model of the micelle aggregates formed

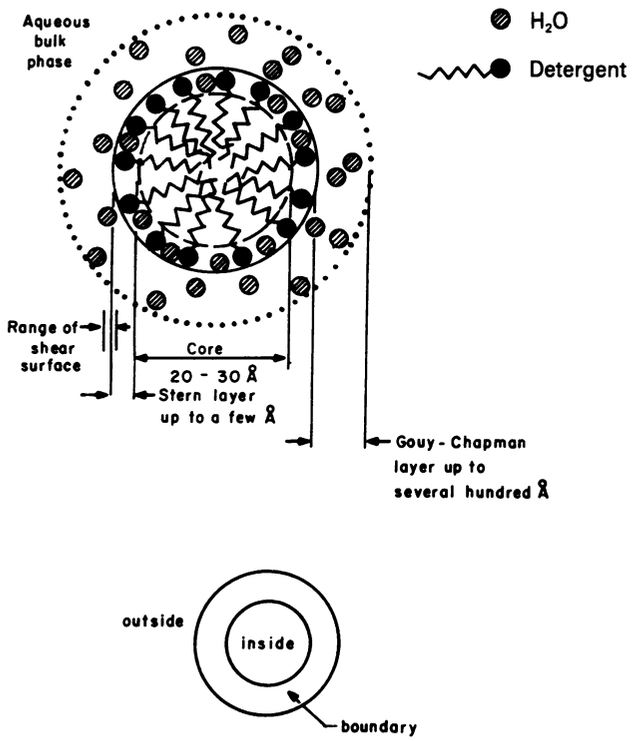

FIG. 9. Schematic model of micelle aggregates formed by addition of $C_{16}NMe_3Cl$ or sodium dodecyl sulfate to water.

from $C_{16}NMe_3Cl$ and sodium dodecyl sulfate at concentrations near the CMC. We assume for simplicity that such micelles have maximal cross sections of the order of 20–30 Å, which correspond to ≈50–100 detergent molecules per micelle. These micelles provide microscopic hydrophobic environments in a fundamentally aqueous medium. The important topological properties of micelles (those geometric properties that are independent of the detailed detergent structure or of the detailed micelle structure) are (*i*) an inside that is hydrophobic and capable of solubilizing organic molecules; (*ii*) a high polar boundary that separates the hydrophobic inside from the bulk aqueous phase, and (*iii*) an outside that consists of the bulk aqueous phase.

Micellar aggregates as hydrophobic cages for the reactions of RPs

The hydrophobic interior of a micelle provides an interesting restricted volume of hydrophobic space (in an otherwise aqueous environment) that is capable of solubilizing an organic substrate. When an organic molecule enters and is solubilized by a micelle, for a certain period of time the solute is captured by the micelle. During this period, the translational freedom of the solute is restricted to the micelle surface or the hydrophobic inside of the micelle.

Consider now a geminate RP that is generated by homolytic cleavage of a molecule that is solubilized in the micelle. This pair will remain geminate until one or both of the radicals escapes into the bulk aqueous phase. Thus, there is a close analogy to the ideas of a solvent cage for a homogeneous fluid solution and the hydrophobic cages provided by micellar aggregates.

In terms of the reactions of RPs, some important quantitative differences exist between solvent cages and micelles. The first difference has to do with the "size" of the two cages. The volume of a solvent cage is, by definition, roughly the size of the encounter RP—i.e., very little free volume is available to the pair so that occupation of the cage is equivalent to being in the state of collision. The volume of a micellar cage, on the other hand, is large enough to allow the geminate pair to separate by distances up to tens of angstroms. The second difference has to do with the time scale for which the RP exists as a geminate pair. For nonviscous organic solutions (e.g., benzene, acetonitrile) at ambient temperature the residence time of a primary geminate pair in a solvent cage is $\approx 10^{-10}$ to 10^{-11} sec. In contrast (7), if the RP possesses six or more carbon atoms, the residence time of the RP in the micelle will generally be $>10^{-6}$ sec.

Effect of micellization on reactions involving RPs

Qualitatively there are a number of general and novel consequences expected when hydrophobic RPs are generated photochemically in micelle environments, including: (*i*) an increase in the efficiency of cage reactions, relative to homogeneous solution, as a result of the relatively slow escape rate of radicals from micellar cages relative to solvent cages, and (*ii*) a decrease in the quantum yield for net reaction in micelles relative to homogeneous solvents as a result of enhanced radical recombination (also a manifestation of the slower escape rate of radicals from micellar relative to solvent cages).

Photolysis of DBK in micellar aggregates

In homogeneous solution, the extent of cage reaction is ≈0% for the photolysis of DBK (8, 9). However, photolysis of aqueous solutions of DBK in micelles results in substantial cage reaction (10). Fig. 10 summarizes the mechanistic conclusions of an extensive series of investigations. The initial ^{3}RP was found to undergo two major reaction pathways: (*i*) ISC to a singlet ^{1}RP, and (*ii*) decarbonylation to produce a secondary caged ^{3}RP′. The ^{1}RP undergoes two combination reactions (within the "cage" provided by the micelle aggregate) to regenerate DBK (path a) and to produce an isomer, 1-phenyl-4-methylacetophenone (path b). The secondary caged ^{3}RP′ undergoes two processes: (*i*) ISC to a ^{1}RP (which then undergoes rapid combination to yield diphenylethane in a cage reaction) and (*ii*) formation of random free radicals.

Fig. 11 provides the type of experimental support that is available for the proposed mechanisms. For a system containing $C_{16}NMe_3Cl$ micelles (cationic), the benzyl radicals that escape into the aqueous phase are scavenged by Cu(II), and $C_6H_5CH_2Cl$ is produced as the product of scavenging. Under comparable photolysis conditions, the yields of DBK lost and of the diphenylethane and benzyl chloride produced were measured as a function of added $CuCl_2$. The data show that scavenging of benzyl radicals was not complete. Only ≈70% of the diphenylethane formed from DBK can be scavenged—i.e., the micelle "cage effect" is ≈30% for recombination of geminate benzyl radicals. On the other hand, the disappearance of DBK was not at all influenced by addition of Cu(II). This means that all the reactions of the primary ^{3}RP are intramicellar—i.e., they occur exclusively in the primary micelle cage. Evidence that some of the primary geminate ^{3}RP radicals eventually undergo recombination to regenerate DBK is available from quantum yield data. The quantum efficiency for disappearance of DBK is ≈30% for the micellar photolysis. Because the T_1 state of DBK has been shown to undergo cleavage to ^{3}RP with close to unit efficiency, ≈70% of the ^{3}RP evidently returns to DBK.

Let us now focus on the recombination reactions of ^{3}RP to yield (after ISC to ^{1}RP) DBK and 1-phenyl-4-methylacetophenone. If the nuclear spins of ^{3}RP can assist in the formation

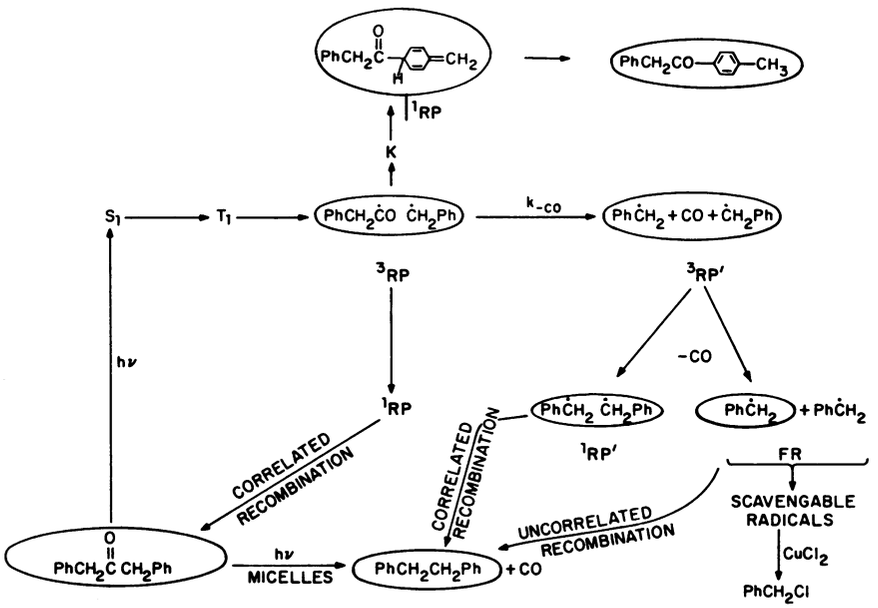

FIG. 10. Reaction scheme for discussion of magnetic effects on the photochemistry of DBK in micellar solution. The encircled species represent micellized molecules or radicals.

of ^{1}RP, then the rate and efficiency of the transformation ^{3}RP $\rightarrow$ ^{1}RP will depend on nuclear spins present in the radical fragments. Suppose that a given RP contained a ^{13}C nucleus which possesses a finite hyperfine coupling to one of the odd electrons in the RP. This RP will enjoy a faster ISC than a RP that contains only ^{12}C nuclei, because the hyperfine interaction will promote ISC via the spin flipping mechanism ($T_+ \rightarrow S$ or $T_- \rightarrow S$) and the spin rephasing mechanism ($T_0 \rightarrow S$). The faster rate of ISC of ^{13}C containing RPs implies that DBK will be regenerated more efficiently from such pairs and that 1-phenyl-4-methylacetophenone will be formed more efficiently from such pairs. In other words (Fig. 12), in an extreme case, ^{3}RP containing ^{13}C will undergo only recombination reaction whereas ^{3}RP containing only ^{12}C will undergo escape reactions (i.e., decarbonylation to form ^{3}RP'). One effect of nuclear spins on the reactions of DKB in micelles will be that the combination products (regenerated DBK and 1-phenyl-4-methylacetophenone) will be enriched in ^{13}C! A second effect of nuclear spins will be that the ^{13}C enrichment will be different at the various distinguishable atoms of DBK and 1-phenyl-4-methylacetophenone and the extent of enrichment at each distinguishable atom will be related to the ^{13}C hyperfine interaction in the RP. A third effect of nuclear spins will be that the efficiency of enrichment will be field dependent, with efficiency decreasing upon application of a high laboratory magnetic field. The latter expectation is the result of an indirect effect of nuclear spins: at zero or low magnetic field all three triplet sublevels of ^{3}RP can undergo hyperfine induced ISC to ^{1}RP, but at a high field (i.e., one whose strength is much stronger than the hyperfine interaction) only $T_0 \rightarrow S$ ISC will occur—i.e., the intersystem crossing of T_+ and T_- to ^{1}RP will be "quenched" at high field and result in a decrease in the efficiency of ^{13}C enrichment. Indeed, all three expectations have been confirmed by experiment (10, 11).

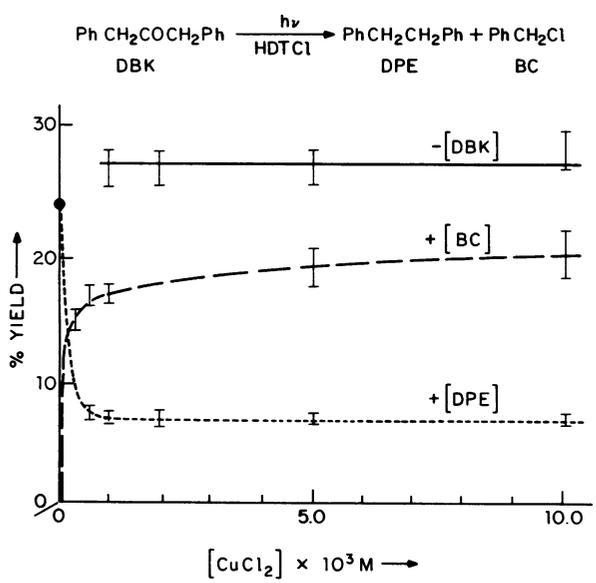

FIG. 11. Plots of disappearance of DBK and appearance of benzylchloride (BC) and diphenylethane (DPE) as a function of $CuCl_2$ concentration for the photolysis of aqueous solution of 10^{-3} M DBK and 0.05 M $C_{16}NMe_3Cl$. Samples were degassed and photolyzed for equal periods of time on a merry-go-round apparatus.

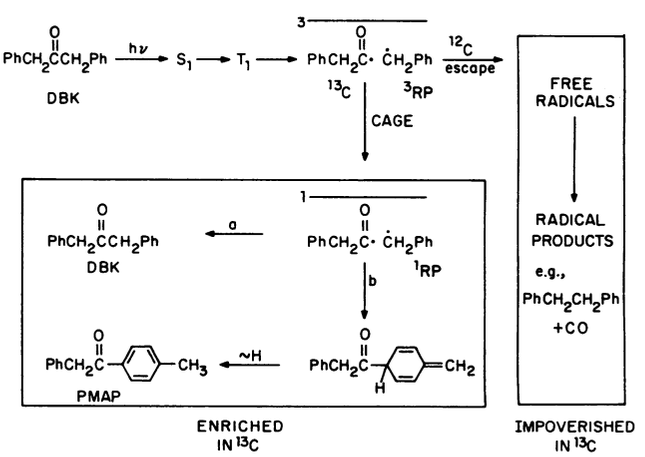

FIG. 12. Strategy for the separation of ^{13}C from ^{12}C based on nuclear spin characteristics. See text for discussion. PMAP, 1-phenyl-4-methylacetophenone.

The magnetic spin isotope effect on recovered DBK

If a $C_{16}NMe_3Cl$ solution of DBK is photolyzed to partial conversion, the residual, recovered DBK is found to be enriched in ^{13}C relative to the initial, unphotolyzed DBK. As a simple demonstration of this effect, consider Fig. 13 which shows the ^1H NMR spectrum of DBK that has been synthetically enriched to 47.6% in ^{13}C at the carbonyl carbon (natural abundance of ^{13}C is 1.1% per carbon atom). A very sensitive test for the ^{13}C enrichment of the carbonyl of DBK is available from integration of the ^{13}C satellites in the ^1H NMR spectrum: the methylene protons of DBK (Fig. 13) with a ^{12}C carbonyl are a singlet (at 3.66 ppm, $CHCl_3$, Me_4Si as internal reference); a doublet centered at the same chemical shift with $J_{^{13}C,H} = 6.5$ Hz is caused by ^{13}C-proton coupling when ^{13}C is contained in the carbonyl. Integration over the singlet and doublet signals allows determination of the ^{13}C content of the carbonyl of DBK. Thus, from the "satellite method" 62 ± 4% ^{13}C is computed to be in the recovered DBK (after 91% conversion). For the DBK recovered after 91% conversion, a quantitative agreement exists between the mass spectrometrically determined mass increase and the ^{13}C enrichment of the carbonyl of DBK determined by ^1H NMR. After mass spectroscopy and ^1H NMR analysis these samples of DBK were subjected to ^{13}C NMR analysis, which also established qualitatively that the predominant ^{13}C enrichment occurs in the carbonyl of DBK (the relative increase of the carbonyl signal corresponds to a 60 ± 5% ^{13}C content). These experiments demonstrate that recovered DBK becomes enriched in ^{13}C as a result of photolysis of DBK in $C_{16}NMe_3Cl$ micelles. These results provide strong evidence that there is a magnetic spin isotope effect in the photolysis of DBK in micellar systems.

In contrast, the photolysis of DBK in nonviscous homogeneous solvents (e.g., benzene) does not result in significant ^{13}C enrichment in the recovered DBK (11, 12, 13). However, photolysis of DBK in viscous solution (e.g., glycerol/tertiary butanol) leads to significant enrichment in the recovered DBK (14).

Thus, the efficiency of isotope separation induced by the spin isotope effect can be markedly enhanced by carrying out the reaction of a RP in an inert environment that provides, in a closed volume or in a restricted space, for the diffusional displacements of a RP.

It has been shown that, for a simple theoretical model (12–14), if the size of the space (R, the radius of an idealized spherical space) and the diffusional rates (D, the diffusion coefficient) in the restricted space satisfy the relationships $k \ll D/R^2$ (where k is the rate of self-reaction of the RP), the efficiency of the magnetic isotope effect is maximal when $k \approx \Sigma a$ where the latter is the sum of the effective magnetic interactions in the RP. For typical organic radicals, $\Sigma a \approx 10^8\ s^{-1}$ and for a nonviscous environment $D \approx 10^{-5}\ cm^2\ s^{-1}$ so that $10^8\ s^{-1}\ a < (10^{-5}/R^2)\ s^{-1}$—i.e., R should be of the order of 10–100 Å.

In terms of a surface diagram (Fig. 14) the role of the micelle may be viewed as providing a boundary which "reflects" the representative point back toward the hyperfine-induced hole after an "overshoot" has occurred. Thus, diffusive escape is temporarily thwarted and a ^{13}C-containing molecule receives extra chances to find a hole which allows return to ground state DBK. Eventually, of course, escape by decarbonylation will take place if neither diffusive escape nor bond formation occurs.

Relationship of ^{13}C enrichment to hyperfine coupling: Site-specific spin effects

In the photolysis of DBK, if ^{13}C nuclear spins control ISC from ^3RP to ^1RP, starting from natural abundance ^{13}C (≈1%) at each

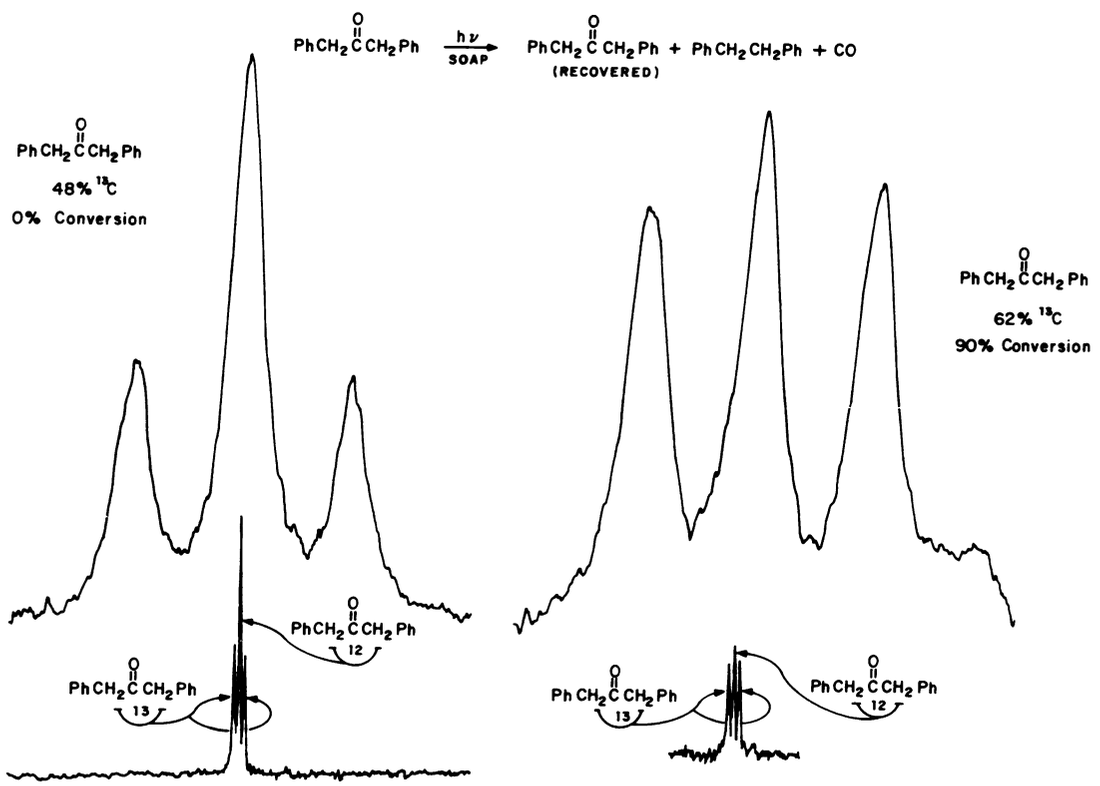

FIG. 13. Comparison of the ^1H NMR spectra of DBK recovered from photolysis in $C_{16}NMe_3Cl$ solution. (*Left*) Methylene resonances of the starting ketone, synthetically enriched in ^{13}C at the carbonyl carbon. (*Right*) Methylene resonances of DBK sample recovered after approximately 90% conversion. See text for discussion.

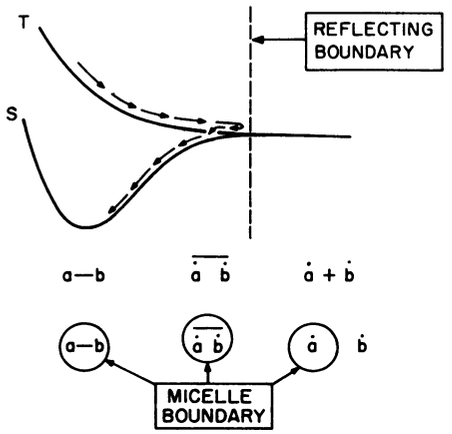

FIG. 14. Schematic representation of the role of micelles as a reflecting boundary for radical fragments in the photolysis of DBK. See text for discussion.

carbon, the ^{13}C enrichment at the various distinguishable carbon atoms in the combination products will be related to the magnitude of the ^{13}C hyperfine constant, a_c, for each of the corresponding carbon atoms in ^3RP.

Table 2 lists the measured, or estimated, values of a_c for the 11 different carbons in ^3RP (see Fig. 15 for numbering system). If, as expected for freely diffusing radical pairs, the ^{13}C enrichment increases monotonically with a_c (15), it is apparent from Table 2 that the ordering of ^{13}C enrichment should be $C_1 > C_{10} > C_{11} > C_{aromatic}$. According to the mechanism in Fig. 12, 1-phenyl-4-methylacetophenone is a combination product which both results after $^3RP \rightarrow {}^1RP$ ISC and which preserves the memory of each distinct carbon atom of ^3RP in its final structure.

Although mass spectroscopic analysis allows determination of the global ^{13}C enrichment in 1-phenyl-4-methylacetophenone, the measurement of ^{13}C enrichment at each carbon is best made by a magnetic resonance method. ^1H NMR ^{13}C satellite intensities, for example, were used as a complement to mass spectroscopy for monitoring the ^{13}C content of specifically labeled DBK and 1-phenyl-4-methylacetophenone samples. However, ^{13}C NMR has the advantage that specific ^{13}C labeling is not required, because small deviations from natural abundance may be determined directly by comparing peak intensities from the sample of interest with those from a standard. The relative enrichments for 1-phenyl-4-methylacetophenone obtained in this way are summarized in Table 2 (19).

The data in Table 2 may be summarized as follows. (*a*) Statistically significant enrichments are obtained for C_1, C_{10}, and C_{11} in the expected order $C_1 > C_{10} > C_{11}$. (*b*) The ^{13}C contents of the other eight carbons varied in this particular sample by <2% from those of the natural abundance. The enrichment S,

Table 2. Relative ^{13}C isotope ratios for 1-phenyl-4-acetophenone by ^{13}C NMR

Carbon*	δ_c, ppm†	S‡	a_c, G
1	197.40	1.23 ± 0.01§	+124¶
2	144.12	(1.00)	−14‖
3	134.93	0.99	0
4	134.25	0.99	+11**
5	129.59	0.99	0
6	129.48	1.01	+12**
7	128.91	0.99	−9**
8	128.79	0.99	0
9	126.95	0.98	0
10	45.60	1.17	+51¶
11	21.84	1.06	+24‖

* See Fig. 15 for number system.
† Chemical shifts relative to $\delta_c^{C_2HCl_3} = 77.27$ ppm. Assignments were made by using selective ^1H decoupling.
‡ Ratio of ^{13}C NMR intensities for analytical and standard samples divided by the ratio for C_2.
§ Error estimate of 1% is 1 SD and represents maximal difference of ratios obtained by curve fitting and spectrum subtraction. See text.
¶ Ref. 15.
‖ Ref. 16.
** Refs. 17 and 18.

however, seems to depend somewhat nonlinearly on a_c. For example, C_{10} seems to be overenriched and C_2 underenriched relative to the magnitudes of their hyperfine couplings. The data nevertheless are in good qualitative agreement with the expectations for a predominant nuclear spin, rather than mass, isotope effect for the formation of 1-phenyl-4-methylacetophenone.

Nuclear spin isotope effects versus classical mass isotope effects

Several features distinguish the effect of nuclear spins on chemical reactions from those due to the "classical" mass isotope effect: (*i*) significant nuclear spin isotope effects will generally be confined to reactions involving radicals and RPs; (*ii*) the nuclear spin isotope effect typically operates at stages that are not rate-limiting, such as self-reactions of RPs; (*iii*) the nuclear isotope effect for "heavy" nuclei (^{13}C, ^{17}O) may reach values approaching and exceeding many tens or hundreds of percent, in contrast to the classical mass isotope effect for heavy nuclei which rarely exceed a few percent; (*iv*) the nuclear spin isotope effect is sensitive to the application of a magnetic field, whereas the classical isotope effect is completely independent of the application of a magnetic field; and (*v*) the magnitude of the magnetic spin isotope effect is related directly to the magnitude of the magnetic moment of the isotope and not to the magnitude of the mass of the isotope.

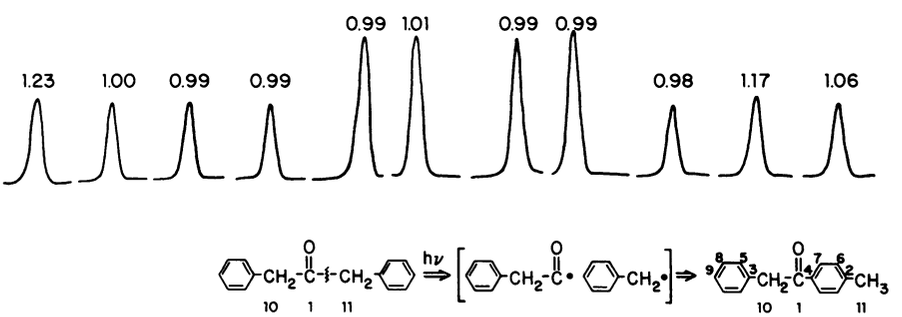

FIG. 15. ^{13}C NMR analysis of the ^{13}C content of 1-phenyl-4-methylacetophenone produced by photolysis of DBK in a micellar media. (*Upper*) Integration according to chemical shifts of the ^{13}C atoms. (*Lower*) Structure showing numbering system for the ^{13}C atoms. See text for discussion.

The influence of an applied field on the effectiveness of nuclear spin interactions

The nuclear electronic hyperfine interaction can serve as a spin rephasing interaction of each odd electron in a RP. This interaction operates even if the radicals are chemically identical but differ in the orientation of their nuclear spins. As a result, the rate of ISC of a RP can depend on the nuclear spin states of the radicals because the orientation of the nuclear spins can influence the rate of rephasing of T_0 to S or of S to T_0. The hyperfine interaction can be viewed as operating along all three directions of an axis system because the nuclear spins can assume various orientations in space. Thus, when the energy separation of the three triplet sublevels is small relative to the hyperfine interaction, the latter is expected to induce transitions between $\{T_+, T_-\}$ and S depends on the strength of an applied external field.

This important influence of an external field on ISC of a RP may be understood as follows. In general, when a perturbation induces a transition between states, its effectiveness depends on the ratio of the strength of the perturbation to the energy separating the states (ΔE) involved in the transition. When the strength of perturbation, P, is comparable or larger than ΔE, the probability of transition is maximal (if all other requirements for transition are met). If $P \ll \Delta E$, (e.g., $P/\Delta E \lesssim 0.1$), the probability of transition is small (even if all other requirements for transition are met). Because the strength of hyperfine couplings are typically <100 G (e.g., $P \lesssim 100$ G), then hyperfine interactions will be ineffective or unable to induce transitions between $\{T_+, T_-\}$ and S, when these states are separated by $\gtrsim$1,000 G (i.e., $\Delta E \gtrsim 1{,}000$ G). This means that at "low fields" (operationally, $P \gtrsim \Delta E$), the three triplet sublevels can undergo hyperfine induced ISC to S, but at "high fields" (operationally $10P < \Delta E$), only T_0 and S can undergo hyperfine-induced ISC (Fig. 16).

Suppose that, starting from a triplet geminate RP, there exists a hyperfine interaction that efficiently induces ISC from $\{T_+, T_-, T_0\}$ to S at low field. In this case, substantial ISC to S may occur and a limiting value of 100% cage reaction may be observed in the limit. At high field, $T_+ \rightarrow$ S and $T_- \rightarrow$ S ISC are "quenched". If mixing of triplet sublevels is also quenched, then only $T_0 \rightarrow$ S ISC can occur. This means that T_+ and T_- will, in the limit, undergo escape processes exclusively, whereas only T_0 and S will undergo cage reaction—i.e., the cage effect will drop from ≈100% at low field to ≈33% at high field.

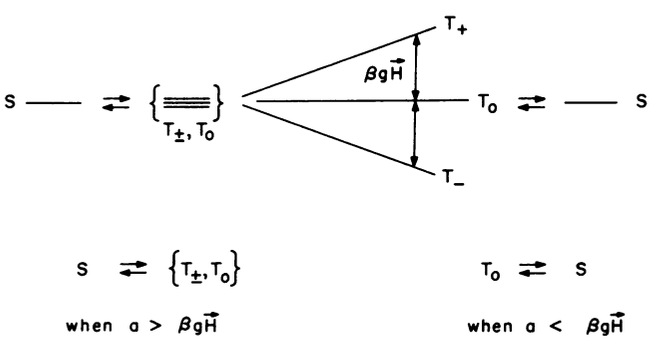

FIG. 16. Schematic representation of the Zeeman interaction βgH on the energetic separation of T_+, T_-, and T_0. When the Zeeman interaction is small relative to other interactions (such as the hyperfine interaction whose strength is given by a, the hyperfine splitting constant), the triplet and singlet states are energetically degenerate, and all three triplet sublevels interconvert with the singlet state. When βgH is large relative to a, only $T_0 \rightarrow$ S ISC occurs. The effect of βgH is to split T_+ and T_- from S energetically and thereby inhibit ISC from or to these sublevels.

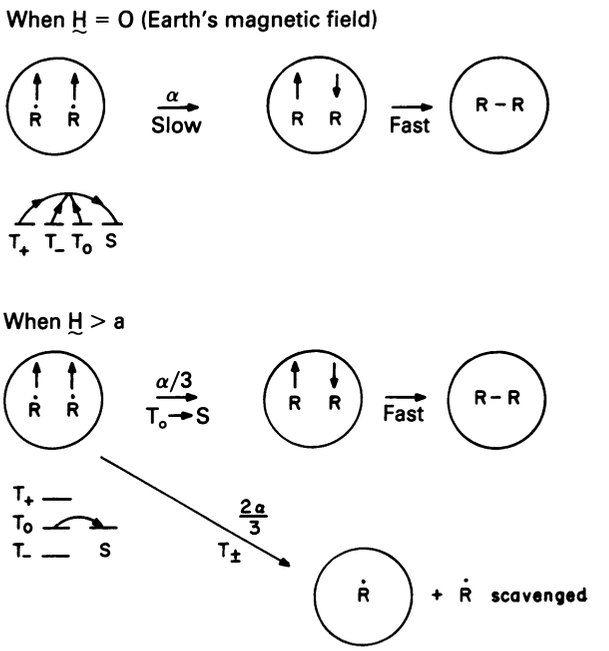

FIG. 17. Schematic representation of the influence of a laboratory magnetic field on the efficiency of the cage reaction of a triplet RP in a micelle. In the earth's field, ISC from T_+, T_-, and T_0 to S is maximal and the fraction α of triplet RPs undergo cage combination. When the applied field is strong enough to inhibit $T_+ \rightarrow$ S ISC, the fraction of cage combination (in the limit) decreases to $\alpha/3$.

Applied magnetic field effects on the reactivity of caged triplet geminate RPs

Let us consider how the above ideas will impact on the behavior of caged triplet geminate RPs (Fig. 17). At low fields all three triplet sublevels will undergo hyperfine coupling-induced ISC to S, whereas at high fields only T_0 will be able to undergo ISC. This means that the percentage cage combination will be dependent on the strength of the applied magnetic field and will initially decrease and then reach a limiting value.

Fig. 18 shows that these expectations are met for the cage efficiency for formation of diphenylethane. Qualitatively, we assume that, from the starting point of ^{3}RP′, a competition is set up between hyperfine-induced ISC and escape from the micelle. At low fields the percentage cage for photolysis in $C_{16}NMe_3Cl$ micelles is 30%, whereas at high fields (>500 G) it is 16%.

An interesting effect of ^{13}C nuclear spins on the percentage cage formation of diphenylethane was found. When DBK enriched 90% in ^{13}C in both CH_2 carbon atoms is photolyzed in $C_{16}NMe_3Cl$ micelles, at low fields the percentage cage jumps from 30% to 45%. This result is interpreted to mean that a geminate benzyl-benzyl RP enriched in ^{13}C at each of the methylene carbons undergoes recombination more efficiently than a geminate benzyl-benzyl RP that contains ^{13}C in natural abundance (≈1%). An important finding is that the percentage cage for DBK that is enriched in ^{13}C at the carbonyl carbon is the same as that for DBK possessing ^{13}C in natural abundance. This is an expected result because the decarbonylation step produces a geminate triplet benzyl-benzyl

$$\overline{C_6H_5{}^{13}\dot{C}H_2\ {}^{13}\dot{C}H_2C_6H_5} \rightarrow 45\%\ \text{cage}$$

$$\overline{C_6H_5{}^{12}\dot{C}H_2\ {}^{12}\dot{C}H_2C_6H_5} \rightarrow 30\%\ \text{cage}$$

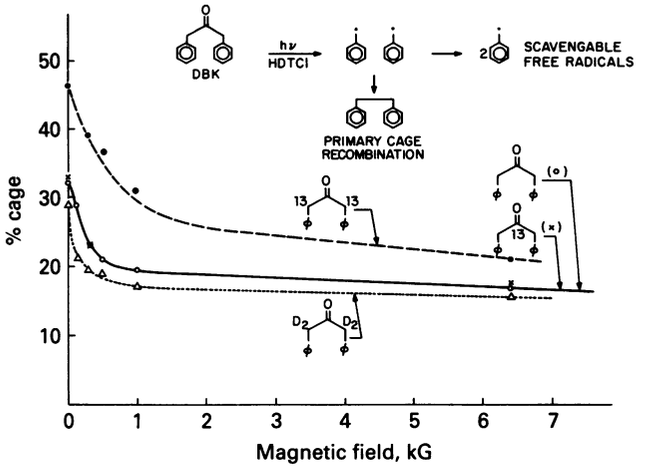

FIG. 18. Cage effects for DBK and isotopically substituted DBKs. Note that ^{13}C substitution at C-1 has no influence on the cage effect, but ^{13}C substitution at C-2 or C-2' causes a substantial increase in the cage effect.

RP which has a natural abundance of ^{13}C. Thus, the efficiency of combination is greater for the RPs enriched in ^{13}C.

Magnetic field effect on the dynamics of benzyl-benzyl RPs in micellar aggregates

The experiments discussed above were concerned with the influence of magnetic fields on the efficiency of recombination of triplet geminate RPs. The suggested mechanism implies that the lifetime of the T_+ and T_- components of the benzyl-benzyl RP should be increased by application of a magnetic field. Fig. 19 shows the results of a flash spectroscopic measurement which confirm this inference. The solid and dashed curves show the decay of benzyl radical absorption after photolysis of DBK with a 16-nsec burst of light from a laser (20). In the very short time domain right after the pulse (≈20 nsec), a slight build-up of benzyl radical absorption is observed (interpreted as a combination of events which decrease benzyl radical absorption and an initially greater increase in benzyl radical absorption due to decarbonylation). For this time domain the decay is similar in the earth's field (0 G) and in a moderate field (3,000 G). After about 100 nsec, the benzyl radical absorption decays motonically. From about 100 nsec to 1,000 nsec, however, there is a dramatic difference in the decay in the presence and absence of a magnetic field. Clearly, the benzyl radical absorption lasts for a much longer period of time in the presence of the field. This result is interpreted to mean that the T_+ and T_- states are inhibited from recombining in the field. Because escape from the micelle aggregate takes >1,000 nsec, the decay profiles shown in Fig. 19 are intramicellar.

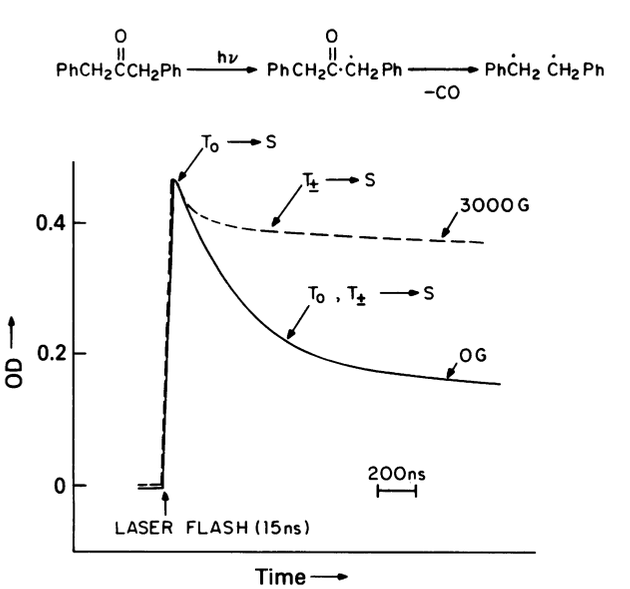

FIG. 19. Time-resolved absorption of benzyl RPs produced by photolysis of DBK in micelles. Dashed line, at 3,000 G; solid line, in the earth's field.

Magnetic spin effects on polymerization

Many industrially important polymerizations are initiated by decomposition of initiators that form RPs. The efficiency of initiation and the molecular weight of these polymerizations often depend on the competition between cage and escape reactions of the RP. Because nuclear spins can influence the competition between the cage and the escape processes, it should be possible to find systems for which nuclear spins can influence the course of polymerizations. Emulsion polymerizations are particularly attractive as candidates for such systems because, at the initial stage of polymerization, micelles swollen with monomer units serve as the loci for the initiation of polymerization (21). Applying the concepts discussed above for magnetic isotope effects and magnetic field effects on the chemistry of triplet RPs, we predict that the efficiency and the molecular weight of emulsion polymers may be significantly influenced by weak magnetic fields such as those associated with magnetic nuclei or with the magnetic stirrers used to agitate solutions of reactants.

The basic idea behind magnetic effects on emulsion polymerizations is shown schematically in Fig. 20. An organic initiator produces a RP in a micelle that is swollen with monomer. One of the radical fragments of this pair initiates polymerization within the micelle. However, because radicals are generated pairwise, a second radical will be present initially in the micelle and will serve as a chain terminator and as a source of initiation inefficiency because "cage" combinations of the RP pair can

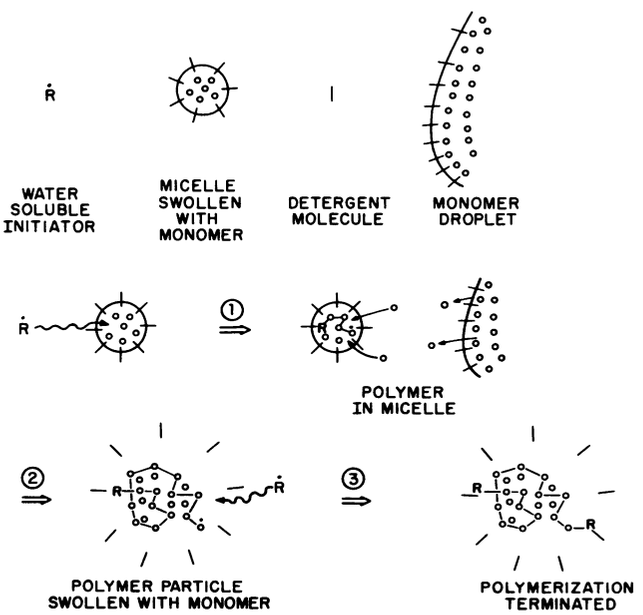

FIG. 20. Schematic representation of the conventional mechanism for emulsion polymerization initiated by a water-soluble initiator. See text for discussion.

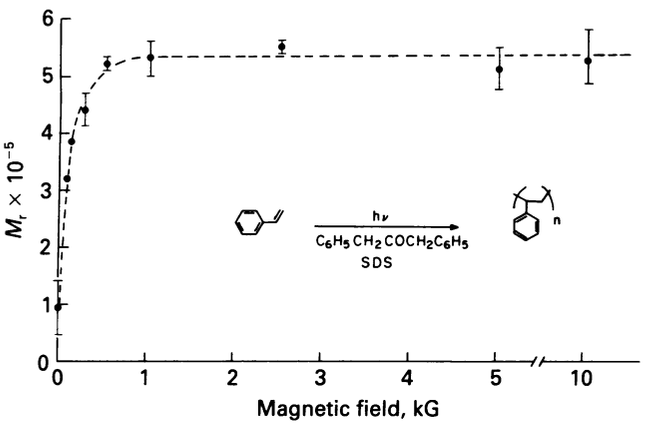

FIG. 21. Magnetic field dependence of the average molecular weight (determined by viscosity measurements) of polystyrene produced by emulsion polymerization photoinitiated by dibenzyl ketone. SDS, sodium dodecyl sulfate.

occur. If, on the other hand, one of the radical fragments escapes the micelle, initiation and propagation will be more efficient and a high molecular weight polymer can be produced.

Because nuclear spins can influence the competition between cage combinations and escape processes of the RP, RPs possessing magnetic isotopes should be less efficient at initiating emulsion polymerization than RPs possessing nonmagnetic isotopes. In addition, weak applied magnetic fields (<1,000 G) should increase the efficiency of initiation and the molecular weight of the emulsion polymer.

Both of these expectations were realized experimentally (22) in the DBK photoinitiated polymerization of styrene and methyl methacrylate in aqueous solutions of sodium dodecyl sulfate. Benzyl radicals initiate these polymerizations. It was found that initiation with $C_6H_5{}^{13}CH_2CO{}^{13}CH_2C_6H_5$ was less efficient and produced lower molecular weight than did initiation with $C_6H_5{}^{12}\dot{C}H_2CO{}^{12}CH_2C_6H_5$. This is interpreted to mean that $C_6H_5{}^{13}\dot{C}H_2$ $^{13}\dot{C}H_2C_6H_5$ RPs undergo more efficient cage reaction relative to escape than do $C_6H_5{}^{12}\dot{C}H_2$ $^{12}\dot{C}H_2C_6H_5$ RPs as expected from Fig. 20.

Both the efficiency of polymerization and the molecular weight of polymer produced in the DBK photoinitiated emulsion were found to depend on the strength of an applied external field. Fig. 21 shows the molecular weight of polystyrene produced in the DBK photoinitiated emulsion polymerization of styrene as a function of applied external magnetic field. The molecular weight increased by ≈500% as the magnetic field increased from the value of the earth's field (≈0.5 G) to a value of several hundreds of gauss; then the effect of magnetic field reached a limiting value, as expected.

It is noted in passing that the magnetic stirrer bars that are used typically to stir solutions generate fields of the order of several hundred gauss. Indeed, the course of the DBK photoinitiated emulsion polymerization of styrene was found to be influenced (rate and molecular weight) by the size of the stirrer bar used to agitate the reaction mixture.

SUMMARY

Under certain conditions, nuclear spins can dramatically influence the rates and efficiencies of reactions of RPs (23–25). Among the key requirements to maximize the influence of nuclear spins on reactions of RPs is to start with a triplet RP in a super cage environment that allows for the correct time and space requirements for the development of singlet character and which encourages return of the fragments to a self-reactive configuration. Another requirement is an escape process for the nonmagnetic RPs. If these conditions are met, a novel means of separating nuclear isotopes (11), based on difference in magnetic moments, and a means of controlling chemical reactions with weak applied magnetic fields (26) become possible.

Prof. James Skinner is thanked for helpful criticism of the manuscript. This work was supported by The National Science Foundation, Department of Energy Grant DE-ACO2-79ER 10362, and Air Force Office of Scientific Research Grant AFOSR-81-0013.

1. Atkins, P. (1976) *Chem. Br.* **12**, 214–218.
2. Buchachenko, A. (1976) *Chem. Rev.* **45**, 375–408.
3. Lawler, R. G. & Evans, G. T. (1971) *Ind. Chim. Belge* **36**, 1087–1089.
4. Buchachenko, A. (1977) *Russ. J. Phys. Chem. (Engl. Transl.)* **51**, 1445–1460.
5. Fendler, J. & Fendler, E. (1975) *Catalysis in Micellar and Macromolecular Systems* (Academic, New York).
6. Turro, N. J., Gratzel, M. & Braun, A. M. (1980) *Angew. Chem. Int. Ed. Engl.* **19**, 675–696.
7. Thomas, J. K., Kalyanasundaran, K. & Grieser, F. (1979) *J. Am. Chem. Soc.* **101**, 279–291.
8. Engel, P. A. (1970) *J. Am. Chem. Soc.* **92**, 6074–6077.
9. Robins, W. K. & Eastman, R. H. (1970) *J. Am. Chem. Soc.* **92**, 6076–6077.
10. Turro, N. J. & Kraeutler, B. (1980) *Acc. Chem. Res.* **13**, 369–377.
11. Turro, N. J. (1981) *Pure Appl. Chem.* **53**, 259–286.
12. Sterna, L., Ronis, D., Wolfe, S. & Pines, A. (1980) *J. Chem. Phys.* **73**, 5493–5499.
13. Tarasov, V. F., Buchachenko, A. L. & Maltsev, V. I. (1981) *Russ. J. Phys. Chem.* **55**, 1921.
14. Buchachenko, A. L., Tarasov, V. F. & Maltsev, V. I. (1981) *Russ. J. Phys. Chem.* **55**, 936–942.
15. Paul, H. & Fischer, H. (1973) *Helv. Chim. Acta* **56**, 1575–1593.
16. Ihrig, A. J., Jones, P. R., Jung, I. N., Lloyd, R. V., Marshall, J. L. & Wood, D. E. (1975) *J. Am. Chem. Soc.* **97**, 4477–4482.
17. Pople, J. A., Beveridge, D. L. & Dobosh, P. A. (1968) *J. Am. Chem. Soc.* **90**, 4201–4209.
18. Albert, K., Dangel, K.-M., Rieker, A., Iwamura, H. & Imahashi, Y. (1976) *Bull. Chem. Soc. Japan* **49**, 2537–2546.
19. Turro, N. J., Chung, C.-J., Lawler, R. G. & Smith, W. J. (1982) *Tetrahedron Lett.* **23**, 3223–3226.
20. Turro, N. J., Chow, M.-F., Chung, C.-J., Tanimoto, Y. & Weed, G. C. (1981) *J. Am. Chem. Soc.* **103**, 4574–4576.
21. Blackley, D. C. (1975) *Emulsion Polymerization* (Wiley, New York).
22. Turro, N. J., Chow, M.-F., Chung, C.-J. & Tung, C.-H. (1980) *J. Am. Chem. Soc.* **102**, 7391–7393.
23. Kaptein, R. (1975) *Adv. Free-Radical Chem.* **5**, 319–380.
24. Closs, G. L. (1971) *23rd International Congress of Pure and Applied Chemistry*, Vol. **4**, pp. 1–19.
25. Atkins, P. & Lambert, T. P. (1975) *Annu. Rev. Chem. Soc. A*, 67–88.
26. Turro, N. J., Chow, M.-F., Chung, C.-J., Weed, G. C. & Kraeutler, B. (1980) *J. Am. Chem. Soc.* **102**, 4843–4845.